Nature of Lowest Electron Transitions in Anionic Polymethine Dyes with Keto-Containing Terminal Groups

O. D. Kachkovsky[1], A. P. Naumenko[2], V. I. Borisyuk[2],
N. V. Obernikhina[3], and Yu. L. Slominskiy[4]

[1]*Institute of Bioorganic Chemistry and Petrochemistry, N.A.S. of Ukraine,*
1, Murmans'ka Str.,
UA-02094 Kyiv, Ukraine
[2]*Taras Shevchenko National University of Kyiv,*
60, Volodymyrs'ka Str.,
UA-03127 Kyiv, Ukraine
[3]*O. O. Bogomolets National Medical University,*
13, Taras Shevchenko Blvd.,
UA-01601 Kyiv, Ukraine
[4]*Institute of Organic Chemistry, N.A.S. of Ukraine,*
5, Murmans'ka Str.,
UA-02660 Kyiv, Ukraine

The complex quantum-chemical and spectral studies of the anionic polymethine dyes with the simplest symmetrical terminal groups and with different-length polymethine chain are performed. As shown, these dyes produce the specific molecular orbitals (MO) positioned nearly the energy gap and located only within the terminal groups. By investigation of the absorption spectra, it is established that the typical highly intensive long-wave-length spectral band is observed and bathochromically shifted upon lengthening of the open conjugated chain; this polymethine band is concerned with the electron transition between the frontier levels of the opposite symmetry. In the contrast, the local MO takes part in so-called quasi-local electron transitions involving also the frontier orbital. The local transitions have small dipole moments, and hence, they do not practically appear in the absorption spectra; however, the local transitions cause the appearance of the non-deep minima in the spectra of the fluorescence-excitation anisotropy.

Проведено комплексне квантово-хемічне та спектральне дослідження аніонних поліметинових барвників з найпростішими симетричними кінцевими групами та з різної довжини поліметиновим ланцюгом. Було показано, що такі барвники ґенерують специфічні молекулярні орбіталі (MO), локалізовані на кінцевих групах і розташовані майже в

енергетичній щілині. Під час вивчення спектрів поглинання досліджуваних сполук спостерігається типова високоінтенсивна довгохвильова смуга, яка батохромно зміщується з подовженням відкритого спряженого ланцюга; така поліметинова смуга пов'язана з переходом електрона між граничними рівнями протилежної симетрії. На відміну від специфічних МО кінцевих груп, локалізовані МО на поліметиновому ланцюзі беруть участь у так званих квазилокальних переходах електронів, задіяних також у граничних орбіталях. Локальні переходи мають малі дипольні моменти; отже, вони практично не з'являються у спектрах поглинання; однак такі переходи спричинюють появу неглибоких мінімумів у спектрах анізотропії збудження флюоресценції.

Key words: anionic polymethine dyes, excitation fluorescence anisotropy spectra, quantum-chemical calculations, excited state, higher electron transitions.

Ключові слова: аніонні поліметинові барвники, спектри збудження анізотропії флюоресценції, квантово-хемічні розрахунки, збуджений стан, вищі електронні переходи.

1. INTRODUCTION

The wide-known ionic (cationic and anionic) polymethine dyes (PMDs) continue to be applied in numerous fields due to their exceptional spectral properties. They form a basis for the design of new effective materials connected with the light conversion [1−4]. In addition, PMDs were found to be convenient objects for new theoretical conceptions and quantum-chemical models to develop [5−10]. Both cationic and anionic PMDs have been established to distinguish, first at all, by a specific distribution of the total positive or negative charge within the chromophore in the ground and excited states; it is not completely and uniformly delocalized along the conjugated chain of p-electrons, but it generates the wave of the alternated partial charges [11], independently on the sign of the total charge [5, 7, 9, 11, 13].

Also, it was demonstrated that going to first excited state is accompanied by the appreciable redistribution of the electron densities in the extensive polymethine chain, so that the densities increase at carbon atoms showing deficit of the electron densities in the ground state, while the electron densities decrease at the atoms bearing of the excessive of the densities in the ground state [2, 12−14].

In the same time, the total charge is delocalized in the both the polymethine chain and two terminal groups; distribution of the charge between the different molecular fragments depends on the chemical constitution of the dyes.

So, the cationic polymethine dyes contain the donor terminal groups, which pull the excess of the electron densities from the both terminal residues to the polymethine chain [12, 15].

In contrast, the acceptor terminal groups in the anionic dyes pull the electron density from the polymethine chain. It can be supposed that degree of the transferring of charge between the molecular fragments in cationic or anionic PMDs should be determined by the donor or acceptor strength of corresponding terminal groups.

Vice-versa, the increasing or decreasing of the fragment charge within the polymethine chain could estimate quantitatively the donor or acceptor strength of the terminal groups [4].

It is logical that charge distribution between the fragments should change upon excitation.

Traditionally, the redistribution of the charge upon the excitation in the PMDs was considered only for the first electron transition [16].

In the same time, it was shown that two lowest electron transitions in the polymethine dyes with the complex conjugated terminal groups, especially, with the comparatively short chain, should be treated as couple transitions so far as they involve two splitting levels and the same soliton level (or level of the charge) (see, for example, review [4] and references therein).

In the cationic dyes, two the highest occupied levels are formed practically by the highest levels of both donor residues and, hence, could treat as donor levels.

In the anionic polymethine dyes, in contrast, the first two excited states involve two lowest vacant levels, which can be considered as acceptor levels.

Thus, the careful study of both the excitation in the polymethine dyes and, hence, the charge redistribution requires the analysis of electron structure of both first and second excited states; exactly, electron transitions in these states determine the most important spectral properties: one- and two-photon absorption, fluorescence, fluorescence excitation anisotropy, nonlinear optical characteristics, *etc*. [17, 18].

This paper presents the results of the quantum-chemical and spectral investigations of the series of the symmetrical and non-symmetrical anionic dyes containing the terminal groups with the variable acceptor strength, taking into consideration both first and second excited states.

2. OBJECTS AND METHODOLOGY

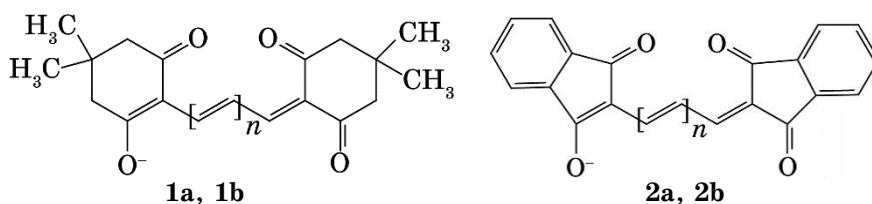*Molecules.* Structural formulas of the studied dyes are shown in Fig. 1.

Fig. 1. Formulae of dyes studied: *a*) $n = 1$; *b*) $n = 2$.

Two vinylogous with different length of the polymethine chain, $n = 1$ and $n = 2$, were investigate to estimate the effect of the lengthening of the chromophore. Both terminal groups contain the generic element: two conjugated diketon groups connected by non-conjugated bridge (compounds **1a, 2b**) and connected by benzene cycle (compounds **2a, 2b**).

Synthetic Procedure. For the compounds **1, 2**, it was described earlier [19, 20].

UV-Vis absorption spectra were recorded on the Shimadzu UV-3100 spectrophotometer in acetonitrile (spectral grade).

Anisotropy of Fluorescence Excitation Spectra. Fluorescence excitation anisotropy measurements are performed using the CM 2203 spectrofluorimeter (Solar, Belarus) in viscous solution (ethylene glycol) to reduce rotational reorientation and at low concentrations ($C \approx 10^{-6}$ M) to avoid reabsorption of the fluorescence. The anisotropy calculated as

$$r(\lambda) = \frac{I_{\parallel}(\lambda) - GI_{\perp}(\lambda)}{I_{\parallel}(\lambda) + G2I_{\perp}(\lambda)}$$

is measured by setting the emission wavelength, typically near the fluorescence maximum, with a fixed polarization. Then, the fluorescence intensity is recorded as a function of excitation wavelength λ at polarizations parallel ($I_{\parallel}(\lambda)$) and perpendicular ($I_{\perp}(\lambda)$) to the emission polarization. *G*-factor expresses sensitivity ratio of detection system for the perpendicular- and parallel-polarized light [21].

Quantum-Chemical Calculations. They were performed using (package Gaussian 03 [22]). The equilibrium geometry of dye molecules in the ground state was optimized by the nonempirical HF/6-31G(*d,p*) and DFT/6-31G(*d,p*)/CAM-B3LYP methods; the electron transition characteristics were calculated by the nonempirical (TD/DFT/6-31G(*d,p*)/CAM-B3LYP) method.

It was found [8, 23, 24] that the calculations of the wavelengths of the electron transitions did not coincide perfectly with the experimental data (that is typical for this approach). However, it is enough to analyse correctly the nature of the electron transitions.

3. RESULTS AND DISCUSSION

3.1. Geometry and Electron Structure of Polymethine Chromophore

The performed calculations give that all four dye molecules, **1a**, **1b** and **2a**, **2b**, are planar, excepting methyl groups, CH_3, which are out molecular plane.

Bond Lengths. According to Dahne's conception [2] of the ideal polymethine state, the lengths of the carbon−carbon bond in the polymethine dyes are equalized maximum, in contrast to the maximum charge alternation. In fact, the calculations give the appreciable alternation of the neighbouring bonds in the chain of the dyes **1a**, **1b** and **2a**, **2b**. It is convenient to estimate the bond-length alternation by following parameter Δl_ν:

$$\Delta l_\nu = \left| l_\nu - l_{\nu-1} \right|, \tag{1}$$

where l_ν is a length of ν-th bond.

The calculated function $\Delta l_\nu = f(\nu)$ for the longer dyes **1b** and **2b** in both ground and first excited states are visually presented in Fig. 2.

Firstly, the calculations give the negligible alternation of the bond lengths, particularly, in the chain middle of both dyes; however, the alternation degree increases somewhat in the excited state. Going from chain centre to its both ends is accompanied by regular increasing of the parameter Δl_ν. In addition, the value Δl_ν for the
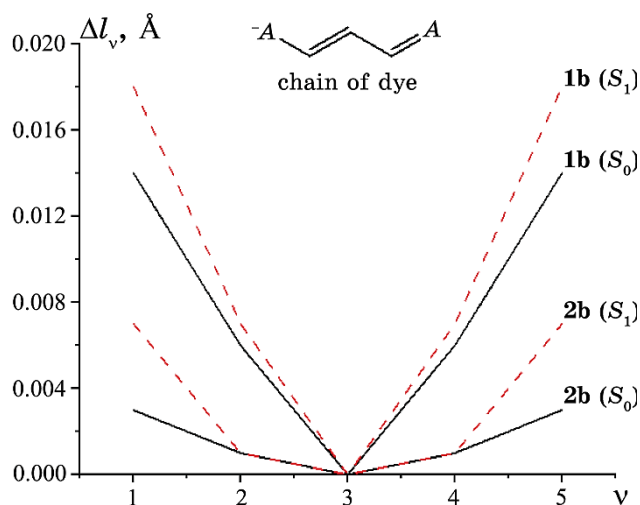

Fig. 2. Bond length alternation, Δl_ν, in the chain of dyes **1b** and **2b**, in ground (S_0) and excited (S_1) states.

bonds nearest to the terminal groups is appreciably sensitive to the acceptor strength (acidity) of residues (compare the dyes **1b** and dye **2b** in Fig. 2).

Atomic Charges. It was already noticed above that total positive or negative charge in the ionic polymethine dyes does not delocalized uniformly in the chromophore, but generates the wave of the alternated electron densities at the carbon atoms along the polymethine chain [11, 15, 25]. Similarly to the bond lengths, to analyse conveniently the dependence of the charge distribution on molecular constitution, it is used the amplitude of the alternation, Δq_μ, calculated as follows:

$$\Delta q_\mu = (-1)^\mu (q_{\mu+1} - q_\mu) \,, \tag{2}$$

where q_μ is the electron density at μ-th atom.

The dependence of the calculated amplitude on the position of the atom in the chain, $\Delta q_\mu = f(\mu)$, for the longer dyes **1b** and **2b** (upon $n = 2$) in both states, ground S_0 and excited S_1, is plotted in Fig. 3.

Figure 3 shows that the degree of the charge alternation, Δq_μ, in the chain of the dyes **1b** and **2b** increases upon going from the terminal group to chain middle, with the exception of the excited state in the dye **2b**, when the parameter Δq_μ is minimal, whereas this parameter Δq_μ decreases in the chain middle. In contrast to the dye **1b**, the alternation of the charges in the chain of other dyes regularly increases in middle of the chromophore; the values for the central atoms is being practically insensitive to the acidity of the
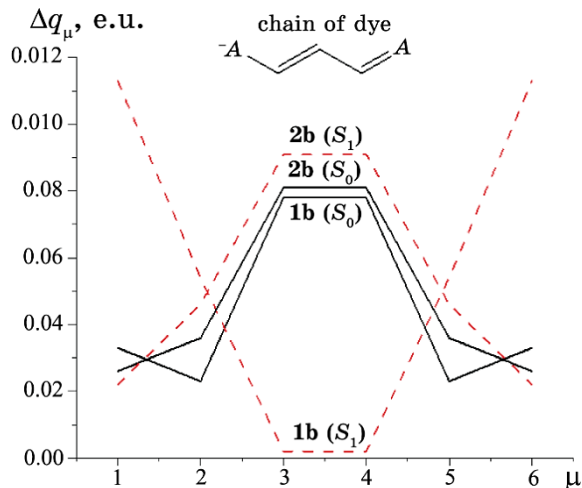

Fig. 3. Charge alternation, Δq_μ, in the chain of dyes **1b** and **2b** in ground (S_0) and excited (S_1) states.

terminal groups: $\Delta q_\mu = 0.080 \pm 0.003$.

And *vice-versa*, the minimum alternation degree follows from the calculation to be reached at both chain ends; the values Δq_μ are appreciably sensitive to the acceptor strength of terminal residues.

Shape of Frontier and Nearest Molecular Orbitals. Now, let us the shape of the frontier (highest occupied molecular orbital—HOMO and lowest unoccupied molecular orbital–LUMO) and nearest MOs, which should involve in the lowest electron transitions and, hence, should be observed in the absorption spectrum in the visible region. Visually, these MOs are plotted in Fig. 4. Firstly, one can see that two types of π-electron MOs appear nearly the electron gap, and, hence, two types of the electron transitions can observe in the spectra. There are π-orbitales delocalized in whole conjugated chromophore (delocalized MOs), so-called local π-MOs located only in the branched terminal groups; additionally, there are *n*-MOs located at the one-co-ordinated oxygen atoms (so-called the lone electron pair—LEP) in both terminal groups with the corresponding electron levels.

Introduction of new vinylene group in the chain ($n = 1 \rightarrow 2$) results in decreasing the energy gap. Besides, the order of the arrangement of the delocalized and local orbitals and LEP can be changed.

One can see that degenerated vacant LUMO+1 and LUMO+2 in all the dyes are exclusively localized within the terminal groups and have their node at the carbon atoms connected with the polymethine chain; thus, the atoms of the chain do not take part in such orbitals. It was shown earlier [4, 26] that the transitions involving the local MOs differ spectrally on the transitions between the totally
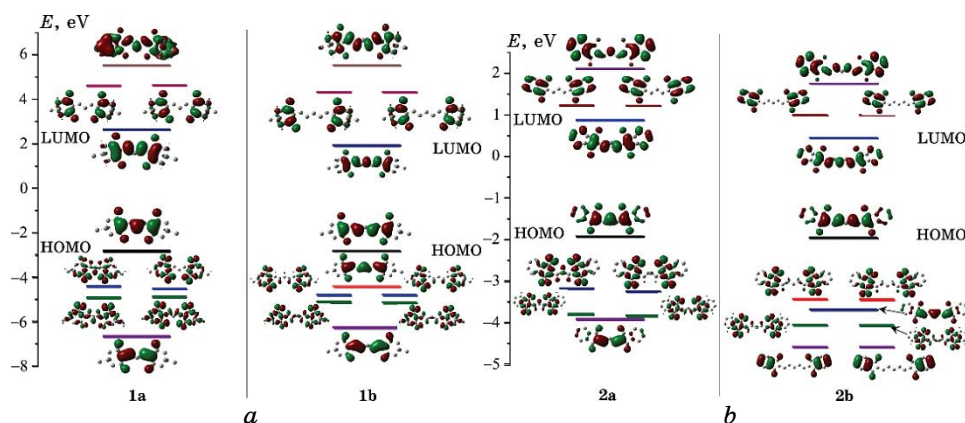

Fig. 4. Energies and shape of frontier and nearest MOs in **1a**, **1b** (*a*) and **2a**, **2b** (*b*).

delocalized orbitals, particularly, by their fluorescence excitation anisotropy.

In addition, all dyes have two pairs of occupied practically n-MOs located at two one-co-ordinated oxygen atoms (partly mixed with σ-MOs). The relative dispositions of the occupied π- and n-levels change upon the chain lengthening. It is natural that such changes of nature of MOs nearly to the energy gap should influence on the nature of the lowest electron transitions.

3.2. Electron Transitions

Correspondingly, the nature of the lowest electron transitions could change depending on the nature of the involved MOs. The contributions of the individual MOs or, more exactly, the contributions of single excited electron configurations $\Phi_{i \to j}$ (involved i-MO and j-MO) in the function of the k-th excited state Ψ_k are determined within the approximation of the configurational interaction as follows:

$$\Psi_k = \sum T_{k,i \to j} \Phi_{i \to j} , \qquad (3)$$

where $T_{k,i \to j}$ is an expansion coefficient; summation runs over all

TABLE 1. Calculated wavelengths (λ), oscillator strength (f) and type of the electron transition of some lowest transitions in dyes **1a** and **1b**.

n	Transition	λ, nm	f	Type	Main configuration
1	$S_0 \to S_1$	383	1.134	$\pi \to \pi^*$	$0.98 \mid \text{HOMO} \to \text{LUMO} >$
	$S_0 \to S_2$	322	0.000	$n \to \pi^*$	$0.85 \mid \text{HOMO–1} \to \text{LUMO} >$
	$S_0 \to S_3$	311	0.000	$n \to \pi^*$	$0.81 \mid \text{HOMO–2} \to \text{LUMO} >$
	$S_0 \to S_4$	296	0.000	$n \to \pi^*$	$0.76 \mid \text{HOMO–3} \to \text{LUMO} >$
	$S_0 \to S_5$	295	0.000	$n \to \pi^*$	$0.71 \mid \text{HOMO–4} \to \text{LUMO} >$
	$S_0 \to S_6$	242	0.180	$\pi \to \pi^*$ Local	$0.90 \mid \text{HOMO} \to \text{LUMO+1} >$
	$S_0 \to S_7$	241	0.033	$\pi \to \pi^*$ Local	$0.96 \mid \text{HOMO} \to \text{LUMO+2} >$
	$S_0 \to S_8$	236	0.049	$\pi \to \pi^* \perp$	$0.82 \mid \text{HOMO–5} \to \text{LUMO} >$
2	$S_0 \to S_1$	440	1.710	$\pi \to \pi^*$	$0.99 \mid \text{HOMO} \to \text{LUMO} >$
	$S_0 \to S_2$	322	0.000	$n \to \pi^*$	$0.85 \mid \text{HOMO–2} \to \text{LUMO} >$
	$S_0 \to S_3$	322	0.000	$n \to \pi^*$	$0.85 \mid \text{HOMO–1} \to \text{LUMO} >$
	$S_0 \to S_4$	303	0.000	$n \to \pi^*$	$0.80 \mid \text{HOMO–4} \to \text{LUMO} >$
	$S_0 \to S_5$	302	0.000	$n \to \pi^*$	$0.77 \mid \text{HOMO–3} \to \text{LUMO} >$
	$S_0 \to S_6$	268	0.019	$\pi \to \pi^* \perp$	$0.99 \mid \text{HOMO–1} \to \text{LUMO} >$
	$S_0 \to S_7$	247	0.185	$\pi \to \pi^*$ Local	$0.91 \mid \text{HOMO} \to \text{LUMO+1} >$
	$S_0 \to S_8$	246	0.023	$\pi \to \pi^*$ Local	$0.95 \mid \text{HOMO} \to \text{LUMO+2} >$

configurations.

The calculated characteristics of some lowest transitions in both dyes **1a** and **1b** are collected in Table 1, while the calculated data for dyes **2a** and **2b** are presented in Table 2.

It follows from Tables 1 and 2 that the first transition, $S_0 \to S_1$, in three dyes is practically described by one configuration with single occupied frontier levels. Only in dye **2b**, the transition involving the frontier levels is seen from Table 2 to be third one; two first transitions involve the local LUMO+1 and LUMO+2. As far as frontier MOs are opposite symmetries (C_{2v} symmetry group), then, the first transition is antisymmetric: $A_1 \to B_1$, and, hence, it is polarized along polymethine chain (see, for example, review [14] and references therein). The calculated comparatively large transition dipole momentum should cause the high intensity of the long-wavelength absorption band.

Going to the higher vinylogous, **1a** $\to$ **1b** and **2a** $\to$ **2b,** is accompanied by the considerable decreasing of the energy of the first electron transition, so that long-wave-length band in absorption

TABLE 2. Calculated wavelengths (λ), oscillator strength (f) and type of the electron transition of some lowest transitions in dyes **2a** and **2b.**

n	Transition	λ, nm	f	Type	Main configuration
1	$S_0 \to S_1$	416	1.556	$\pi \to \pi^*$	$0.99 \mid$ HOMO $\to$ LUMO $>$
	$S_0 \to S_2$	378	0.026	$\pi \to \pi^*$Local	$0.96 \mid$ HOMO $\to$ LUMO+1 $>$
	$S_0 \to S_3$	377	0.036	$\pi \to \pi^*$ Local	$0.95 \mid$ HOMO $\to$ LUMO+2$>$
	$S_0 \to S_4$	349	0.000	$n \to \pi^*$ Local	$0.58 \mid$ HOMO–2 $\to$ LUMO+1 $>$ $-0.61 \mid$ HOMO–1 $\to$ LUMO+2 $>$
	$S_0 \to S_5$	348	0.000	$n \to \pi^*$ Local	$0.59 \mid$ HOMO–2 $\to$ LUMO+2 $>$ $-0.60 \mid$ HOMO–1 $\to$ LUMO+1 $>$
	$S_0 \to S_6$	329	0.000	$n \to \pi^*$	$0.70 \mid$ HOMO–1 $\to$ LUMO $>$
	$S_0 \to S_7$	326	0.005	$\pi \to \pi^* \perp$	$0.92 \mid$ HOMO–5 $\to$ LUMO $>$
2	$S_0 \to S_1$	503	0.527	$\pi \to \pi^*$ Local	$0.84 \mid$ HOMO $\to$ LUMO+2 $>$
	$S_0 \to S_2$	501	0.013	$\pi \to \pi^*$ Local	$0.99 \mid$ HOMO $\to$ LUMO+1 $>$
	$S_0 \to S_3$	496	1.551	$\pi \to \pi^*$	$0.85 \mid$ HOMO $\to$ LUMO $>$
	$S_0 \to S_4$	404	0.000	$n \to \pi^*$	$0.93 \mid$ HOMO-1 $\to$ LUMO $>$
	$S_0 \to S_5$	403	0.000	$n \to \pi^*$	$0.93 \mid$ HOMO-2 $\to$ LUMO $>$
	$S_0 \to S_6$	390	0.000	$n \to \pi^*$ Local $n \to \pi^*$ Local	$0.65 \mid$ HOMO-2 $\to$ LUMO+1 $>$ $-0.66 \mid$ HOMO-1 $\to$ LUMO+2 $>$
	$S_0 \to S_7$	389	0.000	$n \to \pi^*$ Local $n \to \pi^*$ Local	$0.65 \mid$ HOMO-2 $\to$ LUMO+2 $>$ $-0.66 \mid$ HOMO-1 $\to$ LUMO+1 $>$
	$S_0 \to S_8$	364	0.001	$\pi \to \pi^* \perp$	$0.93 \mid$ HOMO $\to$ LUMO + 3 $>$

spectrum should undergo the essential bathochromic shift (so called vinylogous shift).

3.3. Spectral Results

Experimentally, the electron transitions in the polymethine dyes can be detected by their spectra: absorption, fluorescence, and fluorescence excitation anisotropy. Figure 5 shows all three abovementioned spectra of the dyes studied.

As seen, these dyes show the comparative narrow and highly intensive band in the absorption spectra in the visible region. It is well-known that such a band is typical for the ionic polymethine dyes and is concerned with the lowest electron transition involving practically only the frontier levels delocalized along the whole chromophore (see, for example, review [4] and references therein). This agrees with the data in Table 1 discussed above. In addition, the narrow band is observed in the fluorescence spectra with comparatively low Stock's shift that is typical for the polymethine dyes [26].

However, there is an appreciable divergence between the calculated wavelength, λ, in Table 1 and experimental position of the band maximum, λ_{max}, in the absorption spectra (Fig. 5). This defect increases upon lengthening of the polymethine chromophore; the calculated vinylene shifts, $\lambda_{max}(n = 2) - \lambda_{max}(n = 1)$, proves to be regularly lower than the experimental value. Unfortunately, this is the typical imperfection of the time-dependent (TD) DFT method upon calculation of the long linear conjugated systems (especially, their ions) analysed in detail in Refs. [23−25]. We could only optimistically expect that this method reflects correctly the nature of some lowest transitions, $i.e.$, involved MOs, ratio and direction of the higher and first transition moments.

In the excitation fluorescence anisotropy, the relative deep minimum appears in the shorter region nearly at 150−200 nm from the long-wave-length absorption band maximum, when the parameter $r(\lambda)$ reaches the extreme value. This spectrum is similar to the corresponding minimum in the spectra of the cationic polymethine dyes [27]. The similar minimum in the symmetrical cationic cyanine dyes corresponds to the second transition involving the one frontier MO (lowest unoccupied MO, $i.e.$, LUMO) and next high occupied MO (HOMO−1); so far as both MOs are of the same symmetry, then, this transition is polarized perpendicular to the first transition between MOs of the opposite symmetry [27]. In the anionic dye **1a**, perpendicular transition is seen from Table 1 to involve the HOMO−5 and LUMO totally delocalized in the whole main conjugated system. Then, we can propose that this transition is observed in the excita-
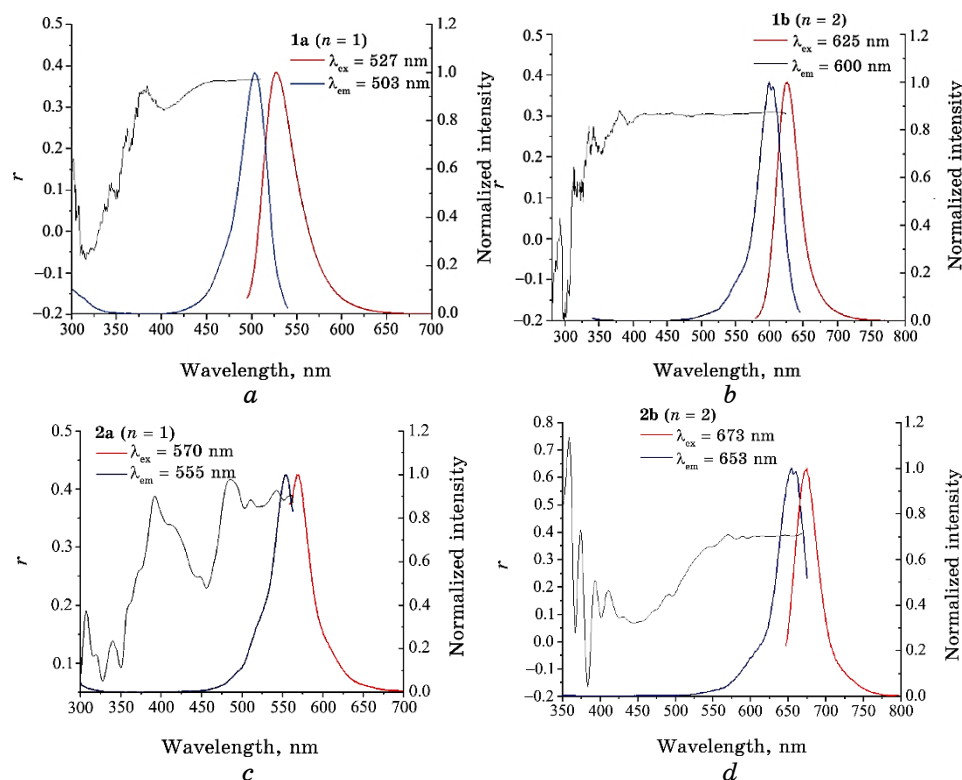
Fig. 5. Spectra of absorption (dark blue) fluorescence (red) and fluorescence excitation anisotropy (black) of the dyes **1a** (*a*), **1b** (*b*), **2a** (*c*), **2b** (*d*).

tion fluorescence anisotropy spectrum as the deep minimum in the region ≈ 320 nm. Between these transitions (involving only the delocalized MOs), the calculations give some transitions of different nature: 4 transitions from 4 occupied *n*-MOs to the same vacant LUMO, as well as 2 transitions from the HOMO to the two degenerated local LUMO+1 and LUMO+2; apparently, they correspond to some non-deep minima in anisotropy spectrum in Fig. 5, *a*.

In the longer dye **1b**, the next occupied delocalized orbital is seen from Fig. 5, HOMO–1; then, the perpendicular transition is seen from Table 1 to involve the HOMO–1 and LUMO delocalized totally. Considering the divergence between calculated and experimental data, we could propose that this transition mixed with the local transitions; apparently, it is a cause of the distortion of the shape of the anisotropy spectrum in Fig. 5, *b*.

The appreciable extending of the π-system in the terminal groups in the dyes **2a, 2b** is accompanied by essential degreasing of the energy gap and, hence, by the shift of the long-wave-length spectral

(both absorption and fluorescence) band connected with the first electron transitions. The calculations predict such shift $= 33$ nm up-on $n = 1$ and 56 nm upon $n = 2$. The experimental measurements give the greater appreciably effect as one can see comparing the corresponding spectra in Fig. 5. Therefore, going from dye **1a** to dye **2a** causes the shift of the long-wave-length band in the absorption spectrum at ≈ 55 nm. Although the performed calculations give the two lowest electron transitions in dye **2b**, which are local (see Table 2), however, the typical polymethine spectral band is observed in the corresponding spectrum (Fig. 5, *d*). Thus, the experimental effect of the extending of the π-system of terminal groups is also ≈ 55 nm (compare corresponding spectra in Fig. 5).

Of course, the similar shifting undergoes also the perpendicular ($A_1 \rightarrow A_1$) electron transition. The most clearly this spectral effect is observed for the short dyes. Comparing the calculated wavelengths of perpendicular $A_1 \rightarrow A_1$ transitions corresponding to dyes **1a** and **2a** (Table 1 and Table 2) gives 110 nm, while the experimental effect is seen from Figures 5, *a* and 5, *c* to be ≈ 130 nm. At the same time, similar estimation of the spectral effect for the local and $n \rightarrow \pi^*$ transitions are difficult because complexity of their spectral manifestations.

4. CONCLUSION

Thus, complex quantum-chemical and spectral study of the anionic polymethine dyes with the symmetrical terminal groups shows that the specific molecular orbitals appear nearly the energy gap located only within the terminal groups. In the absorption spectra, the typical high-intensive long-wave-length spectral band is observed, which is bathochromically shifted upon lengthening the open conjugated chain; this band is concerned with the electron transition between the frontier levels of the opposite symmetry. At the same time, the local MOs produce so-called quasi-local electron transitions involving one of the local MOs and one of the frontier orbital. Because of the small dipole moments, the local transitions do not appear practically in the absorption spectra; however, they cause the appearance of the non-deep minima in the spectra of the fluorescence excitation anisotropy.

REFERENCES

1. A. Mishra, R. K. Behera, P. K. Behera, B. K. Mishra, and G. B. Behera, *Chem. Rev.*, **100**: 1973 (2000); https://doi.org/10.1021/cr990402t
2. G. Orlandi and F. Negri, *Photochem. Photobiol. Sci.*, **1**: 289 (2002); https://doi.org/10.1039/B200178K

3.   S. R. Marder, *Chem. Commun.*, **2**: 131 (2006);
     https://doi.org/10.1039/B512646K

4.   J. L. Bricks, A. D. Kachkovskii, Yu. L. Slominskii, A. O. Gerasov, and
     S. V. Popov, *Dyes Pigm.*, **121**: 238 (2015);
     https://doi.org/10.1016/j.dyepig.2015.05.016

5.   A. B. Ryabitzki, A. D. Kachkovskii, and O. V. Przhonska, *J. Mol. Struct.
     THEOCHEM*, **802**, Nos. 1–3: 75 (2007);
     https://doi.org/10.1016/j.theochem.2006.09.004

6.   J. S. Craw, J. R. Reimers, G. B. Bacskay, A. T. Wong, and N. S. Hush,
     Chem. Phys., **167**: 77 (1992); https://doi.org/10.1016/0301-0104(92)80024-P

7.   J. S. Craw, J. R. Reimers, G. B. Bacskay, A. T. Wong, and N. S. Hush,
     Chem. Phys., **167**: 101 (1992); https://doi.org/10.1016/0301-0104(92)80025-Q

8.   J. Fabian, *Dyes Pigm.*, **84**: 36 (2010);
     https://doi.org/10.1016/j.dyepig.2009.06.008

9.   O. S. Nychyporenko, O. P. Melnyk, O. O. Viniychuk, T. M. Pinchuk-Rugal,
     V. A. Brusentsov, E. L. Pavlenko, O. P. Dmytrenko, N. P. Kulish, and
     O. D. Kachkovsky, *Intern. J. Quant. Chem.*, **114**: 416 (2014);
     https://doi.org/10.1002/qua.24585

10. I. G. Davydenko, Y. L. Slominskiy, N. V. Obernikhina, A. D. Kachkovsky,
     and A. I. Tolmachev, *Chemistry Select.*, **5**, No. 2: 674 (2020);
     https://doi.org/10.1002/slct.201904086

11. K. O. Maiko, I. M. Dmitruk, N. V. Obernikhina, and A. D. Kachkovsky,
     Monatsh. Chem., **151**, No. 4: 559 (2020); https://doi.org/10.1007/s00706-
     020-02572-y

12. A. O. Gerasov, M. P. Shandura, Yu. P. Kovtun, and A. D. Kachkovsky,
     J. Phys. Org. Chem., **21**, No. 5: 419 (2008); https://doi.org/10.1002/poc.1368

13. O. V. Przhonska, H. Hu, S. Webster, J. L. Bricks, A. A. Viniychuk,
     A. D. Kachkovski, and Yu. L. Slominsky, *Chem. Phys.*, **411**: 17 (2013);
     https://doi.org/10.1016/j.chemphys.2012.11.017

14. A. D. Kachkovskiy, *Russian Chemical Reviews*, **66**: 647 (1997);
     https://doi.org/10.1070/RC1997v066n08ABEH000274

15. A. Kachkovsky, N. Obernikhina, Ya. Prostota, A. Naumenko, D. Melnyk,
     and V. Yashchuk, *J. Mol. Struct.*, **1154**: 606 (2018);
     https://doi.org/10.1016/j.molstruc.2017.10.051

16. O. Chernega, S. Levchenko, A. Ryabitskii, A. Gerasov, O. Kachkovskii, and
     Yu. Yagupolskii, *Dyes Pigm.*, **123**: 176 (2015);
     https://doi.org/10.1016/j.dyepig.2015.07.037

17. O. V. Przhonska et al., *Advanced Fluorescence Reporters in Chemistry and
     Biology I. Springer Series on Fluorescence (Methods and Applications)* (Eds.
     A. Demchenko) (Berlin–Heidelberg: Springer: 2010), vol. **8**;
     https://doi.org/10.1007/978-3-642-04702-2_418

18. Ya. Gayvoronsky, A. V. Uklein, A. O. Gerasov, V. V. Garashchenko,
     Yu. P. Kovtun, M. P. Shandura, and O. D. Kachkovsky, *J. Mol. Struct.*,
     1045: 191 (2013); https://doi.org/10.1016/j.molstruc.2013.03.061

19. Yu. L. Slominskiy and I. D. Radchenko, *Chem. Heterocycl. Compd.*, **5**: 711
     (1974).

20. Zh. A. Krasnaya, T. S. Stetsenko, D. G. Gusev, and E. P. Prokof'ev, *Russ.
     Chem. Bull.*, **35**: 1446 (1986); https://doi.org/10.1007/BF00954822

21. J. R. Lackowicz, *Anal. Bioanal. Chem.*, **390**: 1223 (2008);

https://doi.org/10.1007/s00216-007-1822-x

22.   M. Frisch, G. Trucks, H. Schlegel et al., *Gaussian03; Revision B.05* (Pittsburgh, PA: Gaussian Inc.: 2003).

23.   S. Karaca and N. Elmaci, *Comput. Theor. Chem.*, **964**: 160 (2011);
      https://doi.org/10.1016/j.comptc.2010.12.016

24.   D. Jacquemin, Ya. Zhao, R. Valero, C. Adamo, I. Ciofini, and D. G. Truhlar, *J. Chem. Theory Comput.*, **8**: 1255 (2012);
      https://doi.org/10.1021/ct200721d

25.   A. V. Kulinich, N. A. Derevyanko, E. K. Mikitenko, and A. A. Ishchenko, *Phys. Org. Chem.*, **24**, No. 8: 732 (2010); https://doi.org/10.1002/poc.1821

26.   J. Fu, L. A. Padilha, D. J. Hagan, E. W. Van Stryland, O. V. Przhonska, M. V. Bondar, Yu. L. Slominsky, and A. D. Kachkovski, *J. Opt. Soc. Am.*, **24**, No. 1: 56 (2007); https://doi.org/10.1364/JOSAB.24.000056

27.   O. O. Viniychuk, S. M. Levchenko, O. V. Przhonska, O. D. Kachkovsky, Yu. L. Bricks, M. O. Kudinova, Yu. P. Kovtun, Ye. M. Poronik, M. P. Shandura, and O. I. Tolmachev, *J. Mol. Struct.*, **1060**: 30 (2014);
      https://doi.org/10.1016/j.molstruc.2013.12.038